RESEARCH ARTICLE • OPEN ACCESS

Epidemic Dynamics with Nonlinear Incidence Considering Vaccination Effectiveness

Putri Zahra Kamalia and Dipo Aldila

Volume 6, Issue 3, Pages 222–233, September 2025

Received 4 August 2025, Revised 11 August 2025, Accepted 29 August 2025, Published Online 8 September 2025

To Cite this Article : P. Z. Kamalia and D. Aldila,"Epidemic Dynamics with Nonlinear Incidence Considering Vaccination Effectiveness", *Jambura J. Biomath*, vol. 6, no. 3, pp. 222–233, 2025, *https://doi.org/10.37905/jjbm.v6i3.33815*

JOURNAL INFO • JAMBURA JOURNAL OF BIOMATHEMATICS

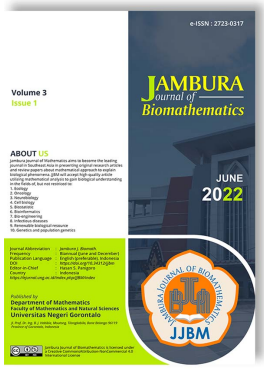

Homepage	:	http://ejurnal.ung.ac.id/index.php/JJBM/index
Journal Abbreviation	:	Jambura J. Biomath.
Frequency	:	Quarterly (March, June, September and December)
Publication Language	:	English
DOI	:	https://doi.org/10.37905/jjbm
Online ISSN	:	2723-0317
Editor-in-Chief	:	Hasan S. Panigoro
Publisher	:	Department of Mathematics, Universitas Negeri Gorontalo
Country	:	Indonesia
OAI Address	:	http://ejurnal.ung.ac.id/index.php/jjbm/oai
Google Scholar ID	:	XzYgeKQAAAAJ
Email	:	editorial.jjbm@ung.ac.id

JAMBURA JOURNAL • FIND OUR OTHER JOURNALS

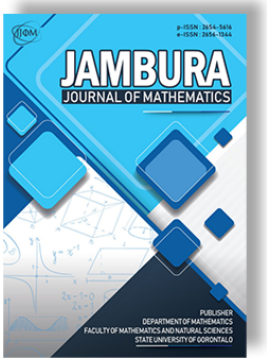

Jambura Journal of Mathematics

Jambura Journal of Mathematics Education

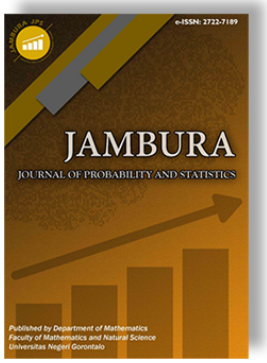

Jambura Journal of Probability and Statistics

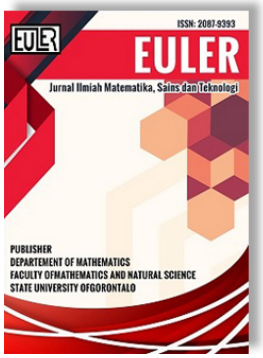

EULER : Jurnal Ilmiah Matematika, Sains, dan Teknologi

Jambura Journal of Biomathematics, Volume 6, Issue 3, Pages 222–233, September 2025 https://doi.org/10.37905/jjbm.v6i3.33815

Research Article

Check for updates

Epidemic Dynamics with Nonlinear Incidence Considering Vaccination Effectiveness

Putri Zahra Kamalia[1,*] **and Dipo Aldila**[1,2]

[1]*Department of Mathematics, Faculty of Mathematics and Natural Sciences, Universitas Indonesia, Depok 16424, Indonesia*
[2]*Innovative Mathematics and Predictive Analytics for Complex System and Technology Laboratory (IMPACT Lab), Universitas Indonesia, Depok 16424, Indonesia*

ARTICLE HISTORY
Received 4 August 2025
Revised 11 August 2025
Accepted 29 August 2025
Published 8 September 2025

KEYWORDS
Nonlinear incidence
Vaccination
Basic reproduction number
Global sensitivity analysis

ABSTRACT. *This paper presents a mathematical model that examines the effect of nonlinear incidence on disease transmission dynamics. Furthermore, we also accommodate newborn and adult vaccination strategy as the prevention strategy to prevent rapid spread of the disease due to nonlinear incidence rate. Assuming a constant population size, the system is reduced to a two-dimensions and nondimensionalized using the average infectious period as the time scale. Analytical results reveal the existence of both disease-free and endemic equilibria, with the possibility of backward bifurcation when the nonlinear incidence parameter exceeds a critical threshold. This implies that disease persistence may still occur even when the basic reproduction number is less than one. Numerical simulations using* `MATCONT` *conducted to visualize the occurrence of both forward and backward bifurcations phenomena. Using COVID-19 parameter values, a global sensitivity analysis via Partial Rank Correlation Coefficient - Latin Hypercube Sampling method indicates that newborn vaccination has a stronger impact on reducing the basic reproduction number. These findings provide important insights for designing effective vaccination strategies and understanding the complex dynamics arising from nonlinear transmission and imperfect immunization.*

1. Introduction

Mathematical models have been widely used by researchers to understand the mechanisms of disease transmission within populations. Since the pioneering work of Kermack and McKendrick in 1927 [1], compartmental models based on disease status have been extensively developed and adapted to various infectious diseases [2, 3]. The global outbreak of COVID-19 in 2019 further amplified the use of mathematical models—not only by mathematicians [4] but also by researchers from other disciplines such as public health, epidemiology, and economics [5, 6]. These models have been employed to predict outbreak trajectories and evaluate potential intervention strategies.

Among the various public health interventions, vaccination remains one of the most effective for controlling and potentially eliminating infectious diseases such as COVID-19, measles, and tuberculosis (TB). However, most vaccines do not provide 100% efficacy. For instance, COVID-19 vaccines generally show efficacy rates ranging from 70% to 95% depending on the type and timing of the dose [7], the measles vaccine achieves around 97% efficacy after two doses [8], and the Bacille Calmette–Guérin (BCG) vaccine for TB shows variable protection between 60% and 80% depending on geographical and demographic factors [9]. Moreover, some vaccines require periodic updates or booster doses due to waning immunity. Therefore, incorporating imperfect vaccine efficacy into disease models is essential when assessing the feasibility of disease eradication through vaccination strategies.

Human behaviour, especially not knowing about or not following disease warnings and health protocols, is another important factor that affects how diseases spread. People with certain infectious diseases can keep doing normal things even if they have symptoms or are at risk of getting sick. This lack of action can greatly speed up the spread of disease, especially in the early stages of an outbreak. The more people who are infected, the more likely it is that people who are susceptible will come into contact with people who are infectious. This happens in a way that isn't always linearly proportional. This phenomenon, which is also called saturation incidence or nonlinear incidence, shows that the number of infected people doesn't always affect the rate of transmission in a straight line [10, 11]. Instead, the number of new infections may rise faster than the number of people who are already infected because of behavioural or biological feedback. People who don't know better may act in ways that make this worse, like skipping vaccinations, avoiding isolation, or ignoring hygiene rules. This can make outbreaks grow faster than simple linear models predict [12]. Because of this, it is important to take these kinds of behaviour changes into account when making realistic models and plans for effective interventions.

Numerous mathematical models have been developed to study the spread of infectious diseases by incorporating vaccination as a primary control intervention. In 2011, Safi and Gumel [13] proposed a mathematical model that considered imperfect vaccination combined with quarantine measures. Their analysis

*Corresponding Author.

Email : *putri.zahra@sci.ui.ac.id* (P. Z. Kamalia)
Homepage : http://ejurnal.ung.ac.id/index.php/JJBM/index / E-ISSN : 2723-0317

Table 1. Description of variables in model (1)

Variable	Description
$S(t)$	Total number of susceptible population at time-t which is vulnerable with disease infection, and not under the impact of vaccination
$V(t)$	Total number of vaccinated individuals at time-t.
$I(t)$	Total number of infected individuals at time-t and ready to spread disease.

revealed the possibility of a backward bifurcation triggered by the imperfection of the vaccine. A more specific application was presented in [14], where the authors implemented a vaccination strategy for malaria. The model parameters were calibrated using incidence data from Papua, Indonesia, and an optimal control framework was employed to evaluate the efficacy of the vaccination strategy in eradicating malaria. In a recent study, Aldila et al. [15] introduced a novel mathematical model to assess the potential impact of the M72/AS01E vaccine on tuberculosis (TB) transmission dynamics. Their model exhibited rich dynamics, including periodic solutions, backward bifurcation, and forward bifurcation with hysteresis. The findings highlighted that the combination of imperfect vaccination and secondary infection pathways—such as relapse and reinfection—could sustain disease transmission even when the basic reproduction number is less than one. More recently, Fatahillah et al. [16] incorporated a saturated infection rate into their vaccination model, uncovering the emergence of backward bifurcation due to saturation effects. This saturation reflects the scenario where the disease transmission rate decelerates as the number of infected individuals increases beyond a certain threshold.

Different with authors in [16] and [17], here in this article we introduce a modified Susceptible – Vaccinated – Infected (SVI) compartmental model that incorporates two key features. The first is the consideration of imperfect vaccination, allowing vaccinated individuals to retain a nonzero probability of infection. The second is the incorporation of a nonlinear incidence rate, which reflects the assumption that as the number of infected individuals increases, the disease spreads more easily—a phenomenon often observed in real-world outbreaks. Through both analytical and numerical approaches, we demonstrate the occurrence of backward bifurcation in the model, primarily induced by the nonlinear transmission mechanism. Furthermore, we perform both local and global sensitivity analyses of the model parameters and the corresponding basic reproduction number.

The structure of the paper is as follows. Section 2 presents the formulation of the mathematical model, including the assumptions involved. In Section 3, we analyze the existence of the disease-free equilibrium and derive the basic reproduction number. Section 4 investigates the existence of the endemic equilibrium, followed by a detailed analysis of backward bifurcation in Section 5. Numerical simulations, including global sensitivity analysis and parameter fitting using COVID-19 data, are discussed in Section 6. Finally, concluding remarks are presented in Section 7.

2. The mathematical model

2.1. *The construction of the mathematical model*

We assume that the population can be divided based on the infection status and vaccination status. Hence, let the human population divided into three compartments as described in Table 1. With the compartment definition shown in Table 1, we define our model as follows.

$$\begin{aligned}
\frac{dS}{dt} &= (1-u_1)\Lambda + \delta V - (1+\alpha I)\beta_1 SI + \gamma I - (u_2+\mu)S,\\
\frac{dV}{dt} &= u_1\Lambda + u_2 S - (1+\alpha I)\beta_2 VI - (\delta+\mu)V,\\
\frac{dI}{dt} &= (1+\alpha I)(\beta_1 S + \beta_2 V)I - (\gamma+\mu)I.
\end{aligned} \tag{1}$$

The model assumptions are as follows:

A1. Assumption for Vaccination:
we assume that the total population N increases due to the natural birth rate, denoted by Λ. We include two types of vaccination in the model, namely newborn vaccination, denoted by u_1, and non-newborn vaccination, denoted by u_2. Hence, $u_1\Lambda$ individuals enter the vaccinated compartment due to newborn vaccination, while the remaining $(1-u_1)\Lambda$, who are not vaccinated, enter the susceptible compartment. Next, we consider non-newborn vaccination, which is administered to individuals in the S compartment. Thus, $u_2 S$ individuals move from the S compartment to the V compartment. Furthermore, we assume that the effect of vaccination is not lifelong. Therefore, there is a dropout from the V compartment to the S compartment at a constant rate δ.

A2. Assumption for infection of susceptible individuals:
we use a nonlinear incidence rate $(1+\alpha I)\beta_1$ to model the infection rate, where β_1 represents the infection rate for the susceptible population, and α reflects the increase in infection rate due to a rising number of infected individuals. With this nonlinear formulation, the infection spreads more rapidly as the number of infected individuals increases.

A3. Assumption for infection of the vaccinated individuals:
we assume that vaccination does not fully protect individuals from infection. The vaccine is assumed to have an efficacy level denoted by ξ, with $\xi \in [0,1]$, where $\xi = 1$ indicates that the vaccine provides 100% protection, and $\xi = 0$ indicates that the vaccine offers no protection at all. Under this assumption, the infection rate for vaccinated individuals is given by $(1-\xi)\beta_1$. Since both ξ and β_1 are constants, we define $\beta_2 := (1-\xi)\beta_1$. Consequently, the infection term for vaccinated individuals is given by $(1+\alpha I)\beta_2 I$, where $\beta_2 \leq \beta_1$.

A4. Assumption for recovery and natural death rate:
we assume that infected individuals can recover from the disease but do not acquire temporary immunity. Hence, all individuals who recover from the I compartment at a rate γ return to the S compartment. Furthermore, we assume that each compartment decreases due to a natural death rate μ.

The description of model parameters are given in Table 2.

Table 2. Description of parameters in model (1)

Parameters with dimension	Description	Dimension	Dimensionless Equivalent
Λ	Recruitment rate per capita	$\frac{\text{human}}{\text{days}}$	-
μ	Natural death rate	$\frac{1}{\text{days}}$	m
u_1	Proportion of newborn get vaccinated	-	c_1
u_2	Non newborn vaccination rate	$\frac{1}{\text{days}}$	c_2
δ	Vaccination waning rate	$\frac{1}{\text{days}}$	d
β_1	Infection rate of the susceptible individuals	$\frac{1}{\text{human} \times \text{days}}$	b_1
β_2	Infection rate of the vaccinated individuals	$\frac{1}{\text{human} \times \text{days}}$	b_2
α	Correction parameter that increases infection rate due to nonlinear impact of infection term	$\frac{1}{\text{human}}$	a
γ	Recovery rate	$\frac{1}{\text{days}}$	-

2.2. *Nondimensionalization of the model*

We assume that the total population in model (1) is constant, hence we have that

$$\frac{dN}{dt} = \Lambda - \mu N = 0 \leftrightarrow \Lambda = \mu N.$$

Let

$$x_1 = \frac{S}{N}, x_2 = \frac{V}{N}, x_3 = \frac{I}{N}, x_1 = 1 - x_2 - x_3, t = \frac{\tau}{\gamma}, m = \frac{\mu}{\gamma},$$
$$c_1 = u_1, c_2 = \frac{u_2}{\gamma}, d = \frac{\delta}{\gamma}, a = \alpha N, b_1 = \frac{\beta_1 N}{\gamma}, b_2 = \frac{\beta_2 N}{\gamma}.$$

Using this assumption, we have the non-dimensional version of model (1) is given as follows:

$$\frac{dx_2}{dt} = c_1 m + c_2(1 - x_2 - x_3) - dx_2 - (1 + ax_3)b_2 x_2 x_3 - mx_2, \tag{2a}$$

$$\frac{dx_3}{dt} = (1 + ax_3)x_3(b_1(1 - x_2 - x_3) + b_2 x_2) - (1 + m)x_3. \tag{2b}$$

The above non-dimensionalized model completed with the following initial conditions:

$$x_2(0) \geq 0, \;\; x_3(0) \geq 0, \;\; \text{with} \;\; x_2(0) + x_3(0) \leq 1.$$

With this nondimension model in hand, we will analyze model (2) instead of the complete model in model (1). In the following section, we will start our mathematical analysis with the calculation of the basic reproduction number and the disease-free equlibrium.

3. The basic reproduction number and the disease-free equilibrium

The first mathematical property we need to examine in our proposed model (model (2)) is its long-term behavior, which allows us to predict the possible final state of the system. To this end, we begin by determining the equilibrium points of model (2).

The first equilibrium point of model (2) is the disease-free equilibrium point, denoted by $\mathcal{E}^*$, and is given by:

$$\mathcal{E}^* = (x_2^0, x_3^0) = (0, 0).$$

Since $x_1 = 1 - x_2 - x_3$, then x_1 in $\mathcal{E}^*$ is given by $x_1^0 = 1$. Therefore, we can see that one possibility of the final state of model (2) is that all individuals in the population are susceptible individuals.

Before we calculate the next equilibrium point, i.e., the endemic equilibrium, it is important to determine a key threshold in epidemic modeling, known as the basic reproduction number. This threshold, often denoted by $\mathcal{R}_0$, represents the expected number of secondary cases generated by a single primary case in a fully susceptible (or 'virgin') population during one infectious period [18]. The term 'virgin population' refers to a population in which all individuals are susceptible to infection. In many epidemic models, $\mathcal{R}_0$ plays a crucial role in determining whether the disease will die out or persist in the population [19–25]. Typically, the disease persists if $\mathcal{R}_0 > 1$, and may die out if $\mathcal{R}_0 < 1$. The expression of the basic reproduction number of model (2) is stated in the following theorem.

Theorem 1. *Model (2) has a respected basic reproduction number given by:*

$$\mathcal{R}_0 = \frac{b_2 c_2 + b_1 m(1 - c_1) + m b_2 c_1}{(1 + m)(m + d + c_2)}.$$

Proof. We use the next-generation matrix method [26] to calculate the basic reproduction number of model (2). First, we compute the Jacobian matrix associated with the infected compartment of model (2), which in our case is x_3. By direct calculation, the Jacobian matrix evaluated at the disease-free equilibrium $\mathcal{E}^*$ is given by:

$$J(\mathcal{E}^*) = \left[\; -1 + b_1 \left(1 - \tfrac{c_1 m + c_2}{c_2 + d + m}\right) + \tfrac{b_2(c_1 m + c_2)}{c_2 + d + m} - m \; \right].$$

Next, we decompose this Jacobian into the transmission and transition matrices of model (2), denoted by F and V, respectively,

such that $J(\mathcal{E}^*) = F + V$. The transmission matrix F includes all terms related to new infections, while all other terms are included in the transition matrix V. Therefore, we obtain:

$$F = \begin{bmatrix} b_1\left(1 - \dfrac{c_1 m + c_2}{c_2 + d + m}\right) + \dfrac{b_2\,(c_1 m + c_2)}{c_2 + d + m} \end{bmatrix},$$
$$V = [-(1+m)].$$

From direct calculation, the next-generation matrix of model (2) is given by:

$$NGM = -FV^{-1} = \left[\frac{b_2 c_2 + b_1 m(1-c_1) + m b_2 c_1}{(1+m)(m+d+c_2)}\right].$$

The basic reproduction number is defined as the spectral radius of the corresponding next-generation matrix. Thus, the basic reproduction number of model (2) is given by:

$$\mathcal{R}_0 = \frac{b_2 c_2 + b_1 m(1-c_1) + m b_2 c_1}{(1+m)(m+d+c_2)}.$$

□

Having the formula of the basic reproduction number in hand, we are ready to determine the local stability criteria of $\mathcal{E}^*$, whih is stated in the following theorem.

Theorem 2. *The disease-free equilibrium $\mathcal{E}^*$ is locally asymptotically stable if $\mathcal{R}_0 < 1$, and unstable saddle node if $\mathcal{R}_0 > 1$.*

Proof. The linearization of model (2) at equilibrium $\mathcal{E}^*$ is given by:

$$\mathcal{J}(\mathcal{E}^*) = \begin{bmatrix} \mathcal{J}_{11} & \mathcal{J}_{12} \\ 0 & \mathcal{J}_{22} \end{bmatrix},$$
$$\mathcal{J}_{11} = -c_2 - d - m,$$
$$\mathcal{J}_{12} = -c_2 - \frac{b_2\,(c_1 m + c_2)}{c_2 + d + m},$$
$$\mathcal{J}_{22} = -1 + b_1\left(1 - \frac{c_1 m + c_2}{c_2 + d + m}\right) + \frac{b_2\,(c_1 m + c_2)}{c_2 + d + m} - m.$$

Hence, the eigenvalues of $\mathcal{J}(\mathcal{E}^*)$ are

$$\lambda_1 = -(m + d + c_2),$$
$$\lambda_2 = -1 + b_1\left(1 - \frac{c_1 m + c_2}{c_2 + d + m}\right) + \frac{b_2\,(c_1 m + c_2)}{c_2 + d + m} - m.$$

From the expression of $\mathcal{R}_0$, solve it with respect to b_1 and substitute it to λ_2, then λ_2 can be rewritten as $\lambda_2 = -(1+m)(1-\mathcal{R}_0)$. Hence, we have that all eigenvalues of $\mathcal{J}(\mathcal{E}^*)$ are negative if and only if $\mathcal{R}_0 < 1$. On the other hand, since λ_1 is always negative and $\lambda_2 > 0$ if $\mathcal{R}_0 > 1$, then we have $\mathcal{E}^*$ is a saddle point if $\mathcal{R}_0 > 1$. Hence the proof is complete. □

Epidemiological Significance of Theorem 1 and 2:
our calculations in Theorem 1 and 2 highlight the importance of $\mathcal{R}_0$ in determining the extinction of the disease. Maintaining the reproduction number below one increases the likelihood of eliminating the disease. As shown in Theorem 1, the formula of $\mathcal{R}_0$ involves model parameters that can be controlled, such as the infection rate, vaccination rate, and others.

4. The endemic equilibrium

The next equilibrium of model (2) is the endemic equilibrium, denoted by $\mathcal{E}^\dagger$. Taking the right hand side of eq. (2a) equal to zero, and solve it respect to x_2 gives

$$x_2 = \frac{c_1 m + c_2(1 - x_3)}{a b_2 x_3^2 + b_2 x_3 + d + m + c_2}.$$

Substitute this to eq. (2b) and collect it respect to x_3 gives:

$$f(x_3) = \sum_{i=0}^{4} a_i x_3^i = 0, \tag{3}$$

where

$$a_4 = a^2 b_1 b_2,$$
$$a_3 = (2-a) a b_1 b_2,$$
$$a_2 = a(b_1(m+d) + b_2(m + c_2 + 1)) + b_1 b_2(1 - 2a),$$
$$a_1 = a m b_1 c_1 - a m b_2 c_1 - a d b_1 - a m b_1 - a b_2 c_2 + d b_1 + m b_1 + m b_2 - b_1 b_2 + b_2 c_2 + b_2,$$
$$a_0 = (1+m)(m + d + c_2)(1 - \mathcal{R}_0).$$

Based on the above analysis, we have the following lemma.

Lemma 1. *Model (2) has an endemic equilibrium which is given by*

$$\mathcal{E}^\dagger = \left(x_2^\dagger, x_3^\dagger\right) = \left(\frac{c_1 m + c_2(1 - x_3^\dagger)}{a b_2 (x_3^\dagger)^2 + b_2 x_3^\dagger + d + m + c_2}, x_3^\dagger\right),$$

where $x_3^\dagger$ is the positive root of the polynomial in eq. (3).

From the expression of polynomial eq. (3), it can be seen that a_4 is always positive, while $a_0 < 0 \iff \mathcal{R}_0 > 1$. Since $x_3^\dagger < 1$, there will always be at least one endemic equilibrium of model (2) when $\mathcal{R}_0 > 1$. This result is stated in the following lemma.

Lemma 2. *Model (2) will always has at least one endemic equilibrium $\mathcal{E}^\dagger$ if $\mathcal{R}_0 > 1$.*

We observe that the number of endemic equilibrium $\mathcal{E}^\dagger$ that may arise from model (2) depends on the number of positive roots of the polynomial in eq. (3). To determine the possible number of positive roots, we apply Descartes' Rule of Signs, as shown in Tables 3 and 4. From Table 4, and based on Lemma 2, we confirm that at least one endemic equilibrium $\mathcal{E}^\dagger$ always exists when $\mathcal{R}_0 > 1$. Moreover, depending on the sign pattern, it is possible to have either one or three endemic equilibrium in this case. On the other hand, Table 3 shows that the disease does not always vanish when $\mathcal{R}_0 < 1$, as it is still possible to have two or even four endemic equilibrium (see rows 1–5 in Table 3). This result highlights the potential for backward bifurcation, where disease persistence can occur even when $\mathcal{R}_0 < 1$. We will continue our analysis on the existence of backward bifurcation on the next section.

Table 3. Descartes' Rule of Signs for the polynomial $\sum_{i=0}^{4} a_i x_3^i = 0$ when $a_0 > 0 \Leftrightarrow \mathcal{R}_0 < 1$

Coefficient Sequence	Sign Changes in eq. (3)	Possible Number of Positive Real Roots
$+,+,+,+,+$	0	0
$+,+,+,-,+$	2	0, 2
$+,+,-,+,+$	2	0, 2
$+,+,-,-,+$	2	0, 2
$+,-,+,+,+$	2	0, 2
$+,-,+,-,+$	4	0, 2, 4
$+,-,-,+,+$	2	0, 2
$+,-,-,-,+$	2	0, 2

Table 4. Descartes' Rule of Signs for the polynomial $\sum_{i=0}^{4} a_i x_3^i = 0$ when $a_0 < 0 \Leftrightarrow \mathcal{R}_0 > 1$

Coefficient Sequence	Sign Changes in eq. (3)	Possible Number of Positive Real Roots
$+,+,+,+,-$	1	1
$+,+,+,-,-$	1	1
$+,+,-,+,-$	3	1, 3
$+,+,-,-,-$	1	1
$+,-,+,+,-$	3	1, 3
$+,-,+,-,-$	3	1, 3
$+,-,-,+,-$	3	1, 3
$+,-,-,-,-$	1	1

5. Existence of backward bifurcation

We will use the Theorem by Castillo-Chavez and Song [27] to prove the existence of backward bifurcation from model (2). For this purpose, let b_1 be the bifurcation parameter with a critical value obtained from $\mathcal{R}_0 = 1$, i.e.

$$b_1^* = \frac{-mb_2c_1 + dm + m^2 + mc_2 - b_2c_2 + d + m + c_2}{d + m(1 - c_1)}.$$

To use this theorem, we need to calculate the following coefficient:

$$\mathcal{A} = \sum_{k,i,j=2}^{3} v_k w_i w_j \frac{\partial^2 f_k}{\partial x_i \partial x_j}(\mathcal{E}^*), \text{ and } \mathcal{B} = \sum_{k,i=2}^{3} v_k w_i \frac{\partial^2 f_k}{\partial x_i \partial b_1}(\mathcal{E}^*),$$

where v and w are the left and right eigenvector of the zero eigenvalue of the Jacobian matrix of model (2), f_2 and f_3 is $\frac{dx_2}{dt}$ and $\frac{dx_3}{dt}$ in model (2), respectively.

Linearization of model (2) around the disease-free equilibrium $\mathcal{E}^*$ evaluated at b_1^* is given by:

$$J = \begin{bmatrix} -(c_2 + d + m) & -\left(c_2 + \dfrac{b_2(c_1 m + c_2)}{c_2 + d + m}\right) \\ 0 & 0 \end{bmatrix}.$$

The eigenvalues are $\lambda_1 = 0$ and $\lambda_2 = -(m + d + c_2)$. Hence, we have 0 is a simple eigenvalue of J, while the other is negative. Hence, we can implement a center manifold approach to analyze the local stability around b_1^*, which is equivalent to $\mathcal{R}_0 = 1$. To use the Castillo Chavez and Song bifurcation theorem, we should determine the left and the right eigenvector respect to the eigenvalue 0. The left eigenvector $W = [w_2 \; w_3]$ should satisfy $WJ = 0$. By direct calculation, we have:

$$w_2 = -\frac{mb_2c_1 + c_2d + mc_2 + b_2c_2 + c_2^2}{(c_2 + d + m)^2}, \; w_3 = 1.$$

On the other hand, the right eigenvector $V = [v_2 \; v_3]^T$ should satisfy $JV = 0$. Similarly, by direct calculation we have:

$$v_2 = 0, \; v_3 = 1.$$

From the derivative of f_2 and f_3, we may calculate $\mathcal{A}$ and $\mathcal{B}$ as follows:

$$\begin{aligned}
\mathcal{A} &= v_3 w_2 w_2 \frac{\partial^2 f_3}{\partial x_2^2}(\mathcal{E}^*) + v_3 w_2 w_3 \frac{\partial^2 f_3}{\partial x_2 \partial x_3}(\mathcal{E}^*) \\
&\quad + v_3 w_3 w_2 \frac{\partial^2 f_3}{\partial x_3 \partial x_2}(\mathcal{E}^*) + v_3 w_3 w_3 \frac{\partial^2 f_3}{\partial x_3^2}(\mathcal{E}^*), \\
&= \frac{1}{(m(1 - c_1) + d)(m + d + c_2)} \left(2(m + 1)(c_2 + d \right. \\
&\quad + m)(-mc_1 + d + m)a + 2dmb_2c_1 + 4m^2b_2c_1 - 2mb_2^2c_1 \\
&\quad + 2mb_2c_1c_2 - 2d^2m - 4dm^2 - 2dmc_2 - 2m^3 - 2m^2c_2 \\
&\quad + 2mb_2c_1 + 2mb_2c_2 - 2b_2^2c_2 - 2d^2 - 4dm - 2c_2d - 2m^2 \\
&\quad \left. -2mc_2 + 2b_2c_2\right), \\
\mathcal{B} &= v_2 w_3 \frac{\partial^2 f_3}{\partial x_2 \partial b_1}(\mathcal{E}^*) + v_3 w_3 \frac{\partial^2 f_3}{\partial x_2 \partial b_1}(\mathcal{E}^*), \\
&= 1 - \frac{c_1 m + c_2}{m + c_2 + d}.
\end{aligned}$$

Since $c_1 \in [0, 1]$, then $\mathcal{B} > 0$. To find a backward bifurcation at $\mathcal{R}_0 = 1$, then $\mathcal{A}$ should be positive, which in this case the following condition should be hold:

$$a > a^*,$$

where

$$\begin{aligned}
a^* = \frac{1}{(1 + m)(m + d + c_2)((1 - c_1)m + d)} &\left((c_1 m + c_2)b_2^2 \right. \\
&+ \left(-dmc_1 - 2m^2c_1 - mc_1c_2 - c_1m - mc_2 - c_2\right)b_2 \\
&\left. + (1 + m)(d + m)(c_2 + d + m)\right).
\end{aligned} \tag{4}$$

With the above calculation, we have the following theorem.

Theorem 3. *Model (2) undergoes a backward bifurcation at $\mathcal{R}_0 = 1$ if $a > a^*$ where a^* is given in eq. (4).*

Epidemiological significance of Theorem 3:
the existence of a backward bifurcation reveals an important insight: the condition $\mathcal{R}_0 < 1$ may not always guarantee disease

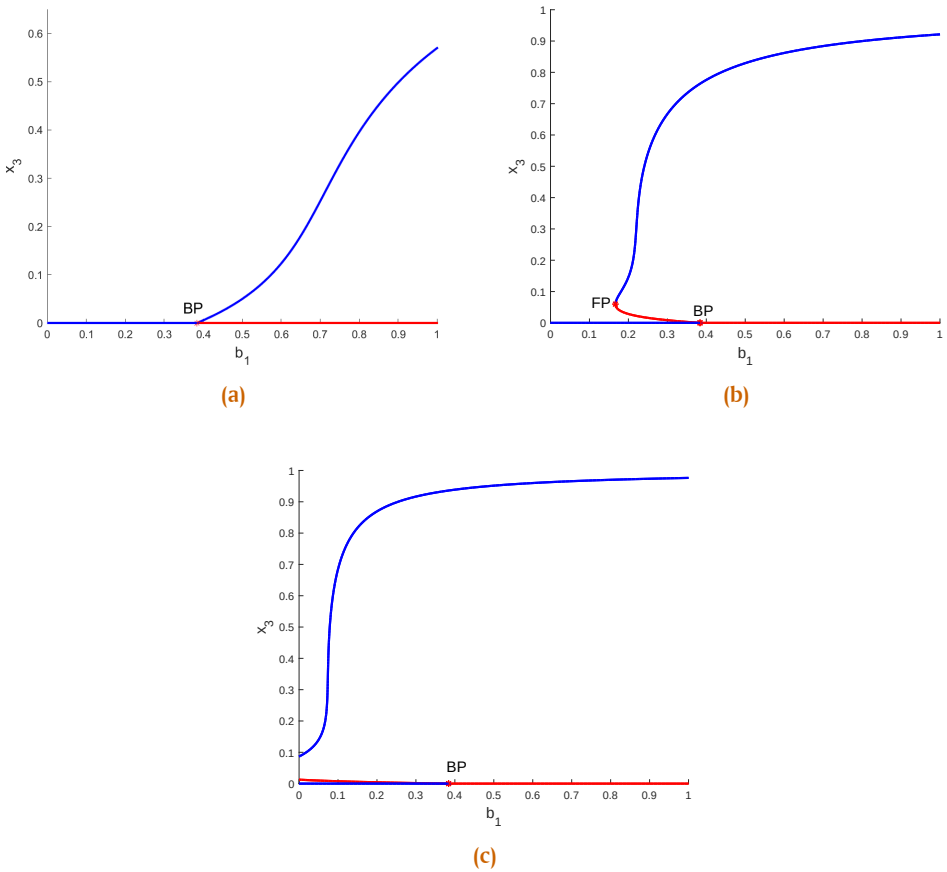

Figure 1. Bifurcation diagram of model (2) at $\mathcal{R}_0 = 1$ shows a forward bifurcation phenomena when $a = 2.102$ in panel (a) and a backward bifurcation when $a = 12.617$ and $a = 42.05$ in panel (b) and (c), respectively. Note that the critical value of a^* is 4.205.

elimination. In our case, the occurrence of backward bifurcation may be driven by a high level of population ignorance regarding disease transmission. The greater the ignorance within the population, the higher the likelihood of disease persistence, even when $\mathcal{R}_0$ has been reduced below unity. This finding highlights the necessity of combining epidemiological control strategies with awareness campaigns or behavioral interventions to ensure successful disease eradication.

6. The numerical experiments

6.1. *Bifurcation diagram*

In this section, we visualized our previous result on the appearance of backward bifurcation when a larger than critical values a^*. To produce the bifurcation diagram, we use `MATCONT`, a MATLAB-based continuation tool. For this purpose, we choose b_1 as the bifurcation parameter and use the following parameter values:

$$d = 0.34,\ m = \frac{14}{23725},\ b_2 = 2.5,\ c_1 = 0.1,\ c_2 = 0.14,$$
$$a = 42.0588.$$

By choosing $b_1 = 1.0$, then we have $\mathcal{R}_0 = 1.436$ which based on previous analytical results, we will have a unique and stable endemic equilibrium $\mathcal{E}^\dagger$, while the disease-free equilibrium $\mathcal{E}^*$ is unstable. With this parameter values, $\mathcal{E}^\dagger$ is given by:

$$(x_2^\dagger, x_3^\dagger) = (0.0000327,\ 0.976259).$$

With the same parameter values, we calculate the critical values a^* that will determine the type of bifurcation that will appears. By direct calculation, we find $a^* = 4.20588$. Hence, if we choose $a > 4.20588$ we will have a backward bifurcation at $\mathcal{R}_0 = 1$, and if $a < 4.20588$, we will have a forward bifurcation at $\mathcal{R}_0 = 1$.

With the above preliminary results, we start our continuation from the endemic equilibrium using `MATCONT` with three different values of a as shown in Figure 1. The first continuation result depicted in Figure 1a by choosing $a = 0.5a^* = 2.102$. It can be seen that when b_1 started from 0, then we only have one equilibrium that appears, denoted by blue line for $x_3 = 0$. This line represents a stable $\mathcal{E}^*$. This stability maintained until it reaches its Branching Point (BP) at $b_1 = 0.383$. BP represent the condition when $\mathcal{R}_0 = 1$. It can be seen that when b_1 reach BP, then $\mathcal{E}^*$ loses its stability, represented by solid red line. In the same time, the endemic equilibrium $\mathcal{E}^\dagger$ started to arise, and maintain it stability as b_1 increases. The next bifurcation diagram is shown in Figure 1b when we choose $a = 3a^* = 12.617$. With this chosen a, we will have a backward bifurcation at $\mathcal{R}_0 = 1$. Different with previous discussion, when we discuss the bifurcation diagram start from smaller b_1, now we discuss the bifurcation diagram starting from bigger value of b_1. When we choose b_1

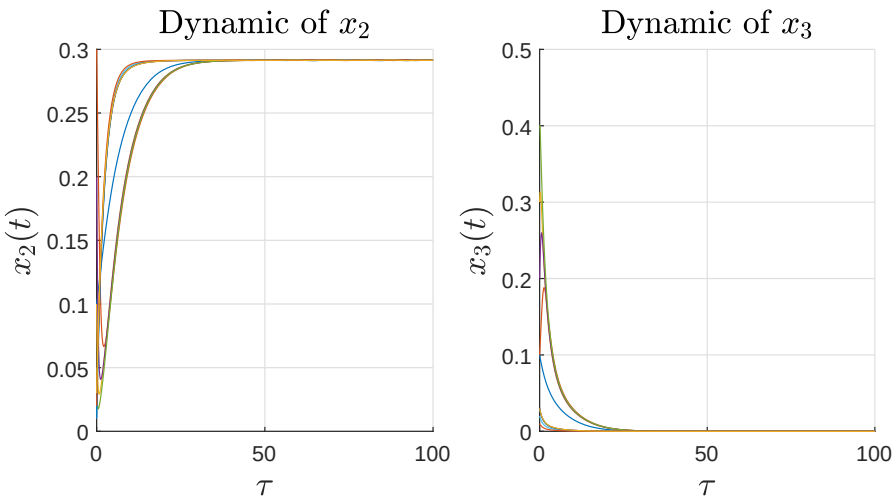

(a)

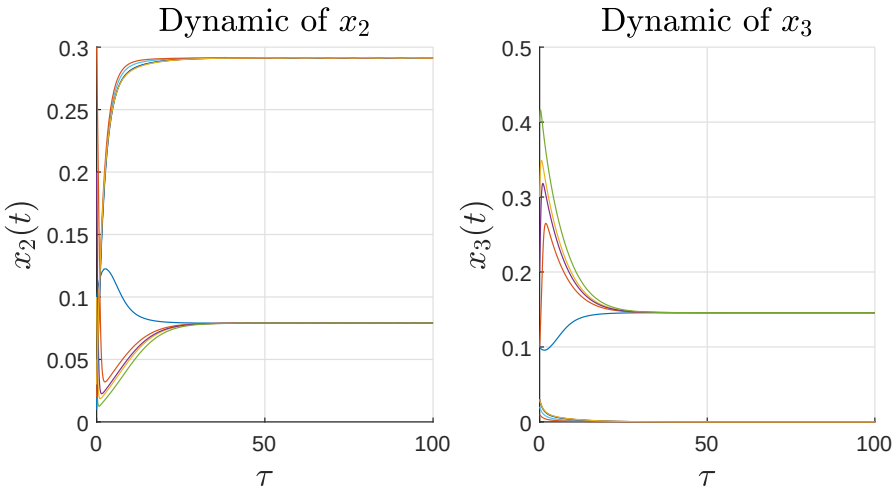

(b)

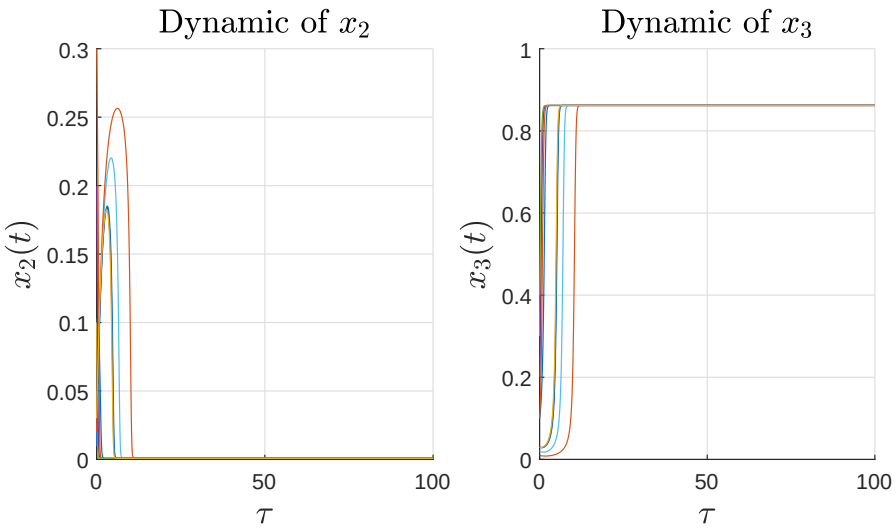

(c)

Figure 2. Dynamic of model (2) respect to bifurcation diagram in Figure 1b with three different value of b_1. Panel (a) depicted dynamic of model (2) with $b_1 = 0.1$, while panel (b) and (c) for b_1 are 0.2 and 0.6, respectively.

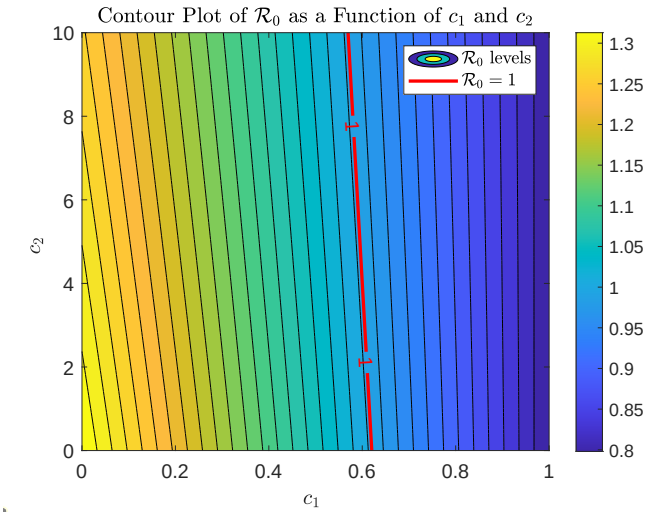

Figure 3. Contour plot of $\mathcal{R}_0$ respect to c_1 and c_2.

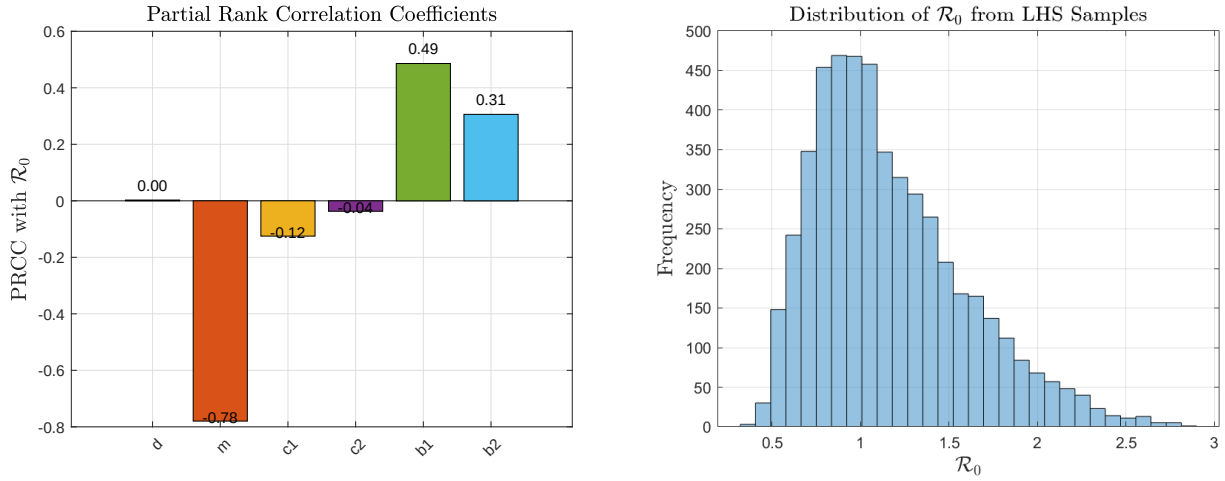

(a) **(b)**

Figure 4. PRCC results for $\mathcal{R}_0$

as in Figure 1b, we have two equilibria that appear. The first equilibrium is $\mathcal{E}^\dagger$, which is stable, while $\mathcal{E}^*$ is unstable. Starting from the blue branch, we track another equilibrium on this branch. Following the path, when b_1 get smaller, we have $\mathcal{E}^\dagger$ keeps maintaing its stability but with smaller size of endemic equilibrium until it reaches the Fold Point (FP) at $b_1 = 0.166$. Passing this point, $\mathcal{E}^\dagger$ loses it stability. As b_1 getting larger from this FP, we have another unstable branch represented with the red curve. As b_1 getting larger on this branch, the smaller endemic equilibrium $\mathcal{E}^\dagger$ stay unstable until it reach the Branching Point BP at $b_1 = 0.383$. Reaching this point, the endemic equilibrium $\mathcal{E}^\dagger$ disappeared. It can be seen that the disease-free equilibrium is stable when b_1 is smaller than BP, and unstable if b_1 is larger than BP. Another important feature that we have from this bifurcation diagram is that it is possible to have two endemic equilibria (stable and unstable) and the disease-free equilibrium when $\mathcal{R}_0 < 1$, to be precise when $b_1 \in$ (FP,BP). In this interval, the long-time behaviour of the system will depend on the initial condition $x_2(0)$ and $x_3(0)$, since we have a bistability phenomena in this interval. This implies that disease eradication cannot be guaranteed solely by reducing $\mathcal{R}_0$ below one and that strong or early intervention is necessary to avoid a rapid escalation in disease prevalence near critical parameter values. Figure 2 represents the dynamic of x_2 and x_3 with respect to three different values b_1 based on the transmission diagram in Figure 1b. In Figure 2a, we choose $b_1 = 0.1$, which gives us only $\mathcal{E}^*$ exist and stable. Hence, all trajectories tends to $\mathcal{E}^*$. In Figure 2b, we choose $b_1 = 0.2$, which is larger than the FP but smaller than BP. With this b_1, we have two stable equilibrium, i.e $\mathcal{E}^*$ and $\mathcal{E}^\dagger$. Hence, we can see in Figure 2b that different initial conditions may give different solution, some of them tends to $\mathcal{E}^*$, while the other tends to $\mathcal{E}^\dagger$. Finally, we choose $b_1 = 0.6$ which is larger than BP, which gives us all solution tends to the endemic equilibrium $\mathcal{E}^\dagger$.

Figure 1c depict a backward bifurcation diagram when we choose an extreme value of a, i.e $10a^*$. With this chosen parameter, we will always have a bistability phenomena for all values $\mathcal{R}_0 < 1$ since the fold point FP appears in the negative region of b_1. In the absence of a fold point in the positive region of b_1, the system exhibits structurally persistent bistability for all $\mathcal{R}_0 < 1$, indicating that disease persistence is not driven by a

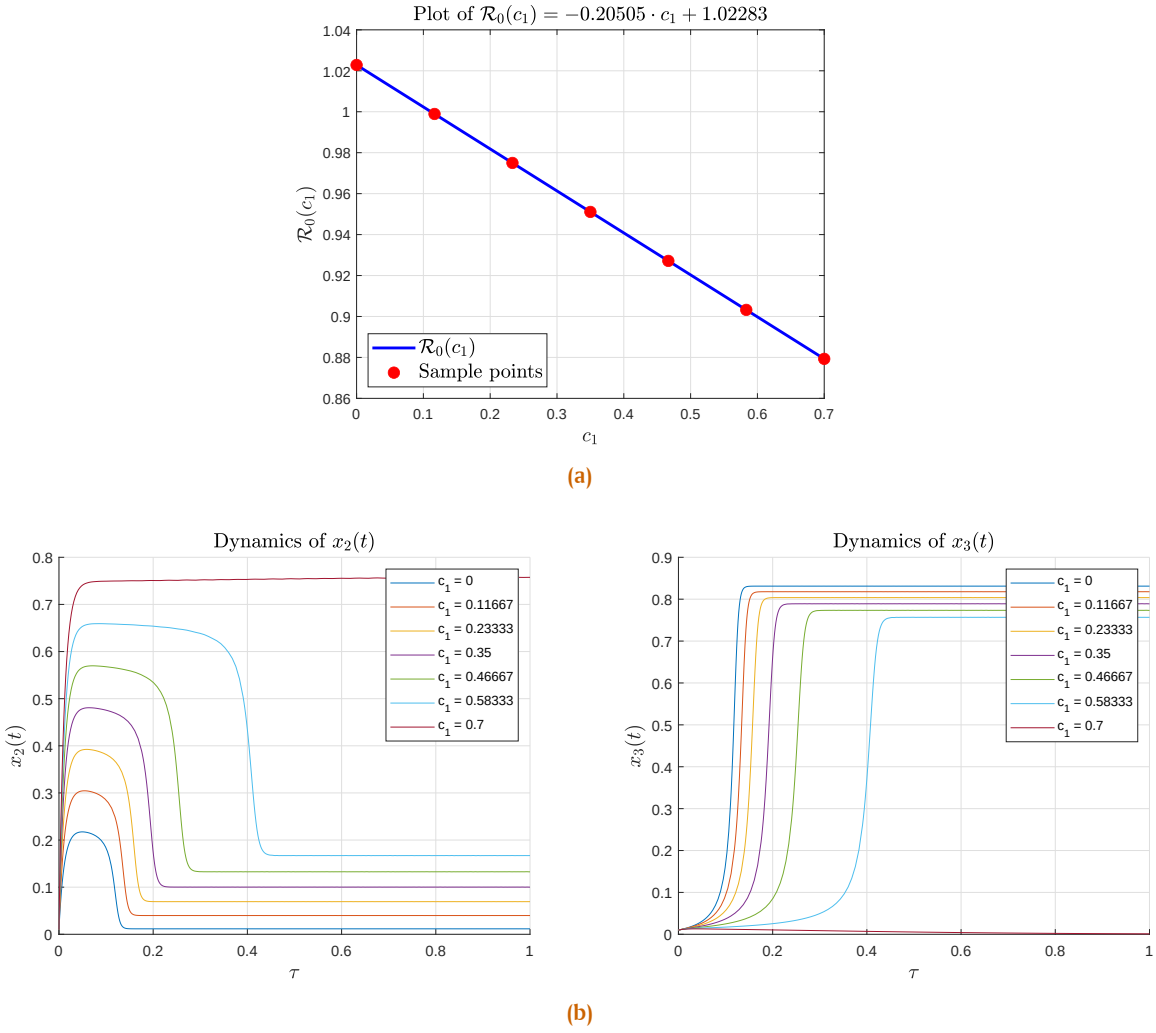

Figure 5. (a) $\mathcal{R}_0$ as a function of c_1, and (b) Dynamic of model (2) respect to the variation of c_1.

saddle-node bifurcation but is inherent to the system dynamics. Consequently, effective eradication requires not only reducing $\mathcal{R}_0$ below one but also altering initial conditions or applying sufficiently strong control to escape the attraction basin of the endemic equilibrium.

6.2. *Sensitivity analysis: Study case on COVID-19*

In this section, we use the following parameter values based on the model introduced by authors in [28] to perform sensitivity analysis on $\mathcal{R}_0$ and dynamic of model (2).

$$\Lambda = \frac{4994000}{(71.85 \times 365)},\ c_1 = 10 \times 0.0344,\ c_2 = \frac{10 \times 0.154}{0.0751},$$
$$m = \frac{1/(71.85 \times 365)}{0.0751},\ b_1 = \frac{10 \times 1.4 \times 10^{-7} \times 4994000}{0.0751},$$
$$b_2 = \frac{10 \times 8.4 \times 10^{-8} \times 4994000}{0.0751}, d = \frac{0.1}{0.0751}.$$

Using the parameter values above, we substitute them into the expression for $\mathcal{R}_0$, keeping c_1 and c_2 as variables. The resulting contour plot of $\mathcal{R}_0$ with respect to c_1 and c_2 is shown in Figure 3. It is evident from Figure 3 that increasing vaccination coverage in both newborns and adults can significantly reduce the value of $\mathcal{R}_0$.

Next, a global sensitivity analysis is conducted using the Partial Rank Correlation Coefficient (PRCC) method combined with Latin Hypercube Sampling (LHS) [29] (see [30–32] for more example on the implementation of this method in epidemic models). We use the parameter values given above and generate sample points within a range of $\pm 50\%$ around each parameter. The results are presented in Figure 4, where Figure 4a shows the global sensitivity of $\mathcal{R}_0$ with respect to each parameter, and Figure 4b displays the distribution of $\mathcal{R}_0$ based on the 10,000 sample points used to produce Figure 4a. It can be observed that the natural death rate plays a crucial role in determining the magnitude of $\mathcal{R}_0$; however, this parameter is typically uncontrollable in practice. Among the controllable parameters, the most influential in our model are b_1, b_2, c_1, c_2, and d, listed in order of decreasing sensitivity. These results indicate that reducing the transmission rates b_1 and b_2 could be effective in lowering $\mathcal{R}_0$ if they can be significantly reduced. Additionally, since the sensitivity values of c_1 and c_2 are negative, increasing the vaccination rates can also help suppress $\mathcal{R}_0$. Newborn vaccination (c_1) has a stronger impact than adult vaccination (c_2).

Next sensitivity analysis is conducted to see the impact of variation of c_1 on the change of $\mathcal{R}_0$ and the dynamic of x_2 and x_3. The results is depicted in Figure 5. In Figure 5a, we confirm

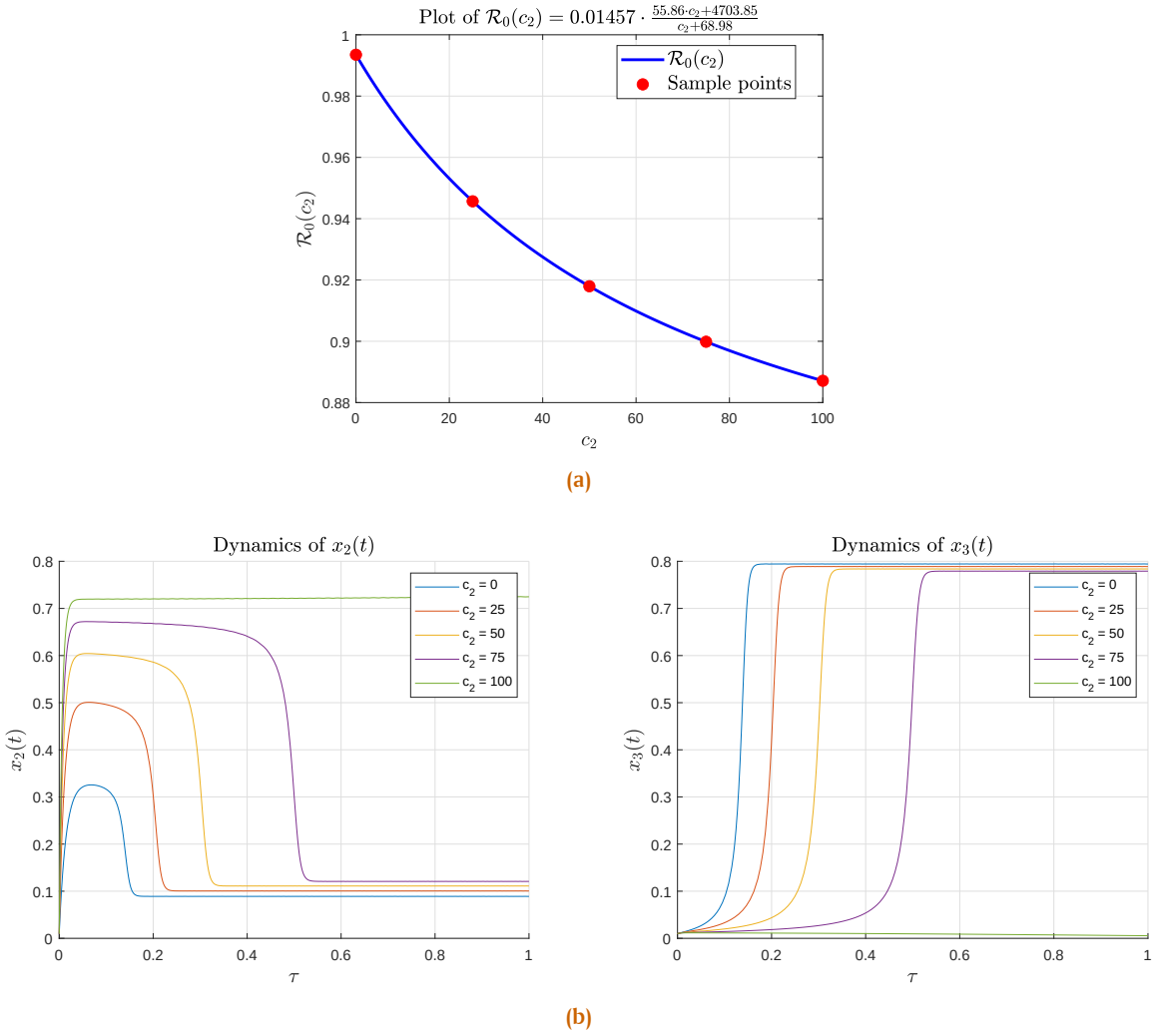

Figure 6. (a) $\mathcal{R}_0$ as a function of c_2, and (b) Dynamic of model (2) respect to the variation of c_2.

our previous sensitivity analysis that increasing c_1 can reduce $\mathcal{R}_0$. With this $\mathcal{R}_0$ as a function of c_1, we choose seven sample points of c_1 (represented by red dot point in panel (a)), and use it to produce the dynamic of x_2 and x_3 as shown in Figure 5b. It can be seen that larger c_1 will increase x_2 and reduce x_3 at equilibrium. With a larger value of c_1, x_2 increases initially until it reaches its peak outbreak, and then starts to decrease and tends to its equilibrium point. On the other hand, smaller vaccination for newborn will increase the number of infected individuals x_3.

A final sensitivity analysis is conducted to examine the impact of the adult vaccination rate, c_2, on the magnitude of $\mathcal{R}_0$ and the dynamics of x_2 and x_3. The results are shown in Figure 6. Figure 6a demonstrates that increasing c_2 leads to a reduction in $\mathcal{R}_0$. However, unlike the effect of c_1, which shows a linear decrease in $\mathcal{R}_0$, the relationship between c_2 and $\mathcal{R}_0$ is nonlinear—exhibiting a rapid decrease at smaller values of c_2 and a slower decline as c_2 becomes larger. Five sample points of c_2, indicated by red dots in Figure 6a, are selected to illustrate their effects on the dynamics of x_2 and x_3, as presented in Figure 6b. Similar to the influence of c_1, increasing the adult vaccination rate results in higher values of x_2 and a reduction in x_3. These findings highlight the potential role of adult vaccination in decreasing the number of infected individuals in the population.

7. Conclusions

In this paper, we propose a mathematical model to investigate the impact of imperfect vaccination and nonlinear incidence on disease dynamics. The nonlinear incidence function is used to capture the potential for accelerated disease transmission as the number of infected individuals increases, a phenomenon commonly observed in real-world epidemics due to behavioral or saturation effects. The model is formulated as a system of ordinary differential equations, involving the compartments: susceptible, vaccinated, and infected individuals. Two vaccination strategies are considered: newborn vaccination and adult vaccination. We assume that recovered individuals do not develop lasting immunity and may become reinfected immediately after recovery. Consequently, the recovered compartment is excluded from the model.

Assuming a constant total population, the model is reduced to a two-dimensional system. Additionally, the system is nondimensionalized by rescaling parameters and time, where one unit of time corresponds to the average infectious period. The analysis of the model reveals the existence of two types of equilibria: the disease-free equilibrium and the endemic equilibrium. The disease-free equilibrium is locally asymptotically stable when the basic reproduction number $\mathcal{R}_0 < 1$, and unstable when $\mathcal{R}_0 > 1$.

Interestingly, the model can exhibit multiple endemic equilibria. Moreover, we identify the occurrence of a *backward bifurcation* when the nonlinear incidence parameter exceeds a critical threshold. In this scenario, the system admits a stable endemic equilibrium even when $\mathcal{R}_0 < 1$, complicating disease eradication efforts [33–35].

Several numerical experiments were conducted to support the analytical findings. A bifurcation diagram was generated using `MATCONT`, illustrating the potential for both forward and backward bifurcation in the model. In particular, the results highlight the possibility of bistability when $\mathcal{R}_0 < 1$, provided the nonlinear infection parameter exceeds a critical threshold. This suggests that even when the basic reproduction number is below one, the disease may persist if initial conditions are not properly controlled. Furthermore, a global sensitivity analysis was performed using the Partial Rank Correlation Coefficient combined with Latin Hypercube Sampling (PRCC-LHS) to examine how model parameters influence the basic reproduction number $\mathcal{R}_0$. The analysis reveals that newborn vaccination has a more significant impact on reducing $\mathcal{R}_0$ compared to adult vaccination. This result underscores the importance of implementing effective newborn vaccination programs, which have been widely adopted for controlling various infectious diseases.

In conclusion, our study demonstrates that accounting for nonlinear transmission and imperfect vaccination in epidemiological models provides critical insights into the dynamics of disease spread. The presence of backward bifurcation emphasizes the need for early and sustained control strategies, while sensitivity analysis reinforces the value of prioritizing newborn vaccination to achieve disease elimination. Although the formulated model present for a general type of disease, the proposed model provides a flexible framework that can be adapted to various infectious diseases with a similar transmission mechanism. This generality ensures broader applicability while allowing future studies to calibrate the model to specific diseases, such as seasonal influenza, tuberculosis, or other direct-contact diseases that can be prevented through vaccination.

For future research, our model may be improved in several directions. One idea is to include non-homogeneous vaccination rates, for example by differentiating between adult, child, and newborn vaccination. Another possible direction is to formulate vaccination interventions as an optimal control problem, in order to address budget limitations during pandemic situations. Real data calibration, as well as incorporating stochasticity and uncertainty factors, could also be considered to better capture the possibility of random outbreaks.

Author Contributions. **Kamalia, P. Z.**: Conceptualization, methodology, formal analysis, investigation, writing—original draft preparation, writing—review and editing, project administration, funding acquisition. **Aldila, D.**: Conceptualization, methodology, software, formal analysis, investigation, resources, writing—original draft preparation, writing—review and editing, visualization.

Acknowledgement. The authors are thankful the editors and reviewers who have supported us in improving this manuscript.

Funding. This research is funded by Universitas Indonesia with PUTI Research Grant Scheme 2025 (ID: PKS-218/UN2.RST/HKP.05.00/2025).

Conflict of interest. The authors declare no conflict of interest.

Data availability. Not applicable.

References

[1] W. O. Kermack and A. G. McKendrick, "A contribution to the mathematical theory of epidemics," *Proceedings of the Royal Society of London. Series A*, vol. 115, no. 772, pp. 700–721, 1927. DOI:10.1098/rspa.1927.0118

[2] H. W. Hethcote, "The mathematics of infectious diseases," *SIAM Review*, vol. 42, no. 4, pp. 599–653, 2000. DOI:10.1137/S0036144500371907

[3] F. Brauer, "Compartmental models in epidemiology," in *Mathematical epidemiology*, Berlin: Springer, 2008. DOI:10.1007/978-3-540-78911-6_2

[4] D. Aldila *et al.*, "A mathematical study on the spread of COVID-19 considering social distancing and rapid assessment: The case of Jakarta, Indonesia," *Chaos, Solitons & Fractals*, vol. 139, p. 110042, 2020. DOI:10.1016/j.chaos.2020.110042

[5] M. Chinazzi *et al.*, "The effect of travel restrictions on the spread of the 2019 novel coronavirus (covid-19) outbreak," *Science*, vol. 368, no. 6489, pp. 395–400, 2020. DOI:10.1126/science.aba9757

[6] X. Wei *et al.*, "Assessing the effectiveness of the intervention measures of COVID-19 in China based on dynamical method," *Infectious Disease Modelling*, vol. 8, no. 1, pp. 159–171, 2023. DOI:10.1016/j.idm.2022.12.007

[7] F. P. Polack *et al.*, "Safety and efficacy of the bnt162b2 mrna covid-19 vaccine," *New England Journal of Medicine*, vol. 383, no. 27, pp. 2603–2615, 2020. DOI:10.1056/NEJMoa2034577

[8] CDC, "Measles (rubeola): For healthcare professionals," https://www.cdc.gov/measles/hcp/index.html, 2022, Accessed on 18 July 2025.

[9] B. Trunz, P. Fine, and C. Dye, "Effect of bcg vaccination on childhood tuberculous meningitis and miliary tuberculosis worldwide: a meta-analysis and assessment of cost-effectiveness," *The Lancet*, vol. 367, no. 9517, pp. 1173–1180, 2006. DOI:10.1016/S0140-6736(06)68507-3

[10] D. vAldila, C. A. Puspadani, and R. Rusin, "Mathematical Analysis of the Impact of Community Ignorance on the Population Dynamics of Dengue," *Frontiers in Applied Mathematics and Statistics*, vol. 9, p. 1094971, 2023.

[11] V. Capasso and G. Serio, "A generalization of the kermack-mckendrick deterministic epidemic model," *Mathematical Biosciences*, vol. 42, no. 1–2, pp. 43–61, 1978. DOI:10.1016/0025-5564(78)90006-8

[12] S. Funk, M. Salathé, and V. A. Jansen, "Modelling the influence of human behaviour on the spread of infectious diseases: a review," *Journal of the Royal Society Interface*, vol. 7, no. 50, pp. 1247–1256, 2010. DOI:10.1098/rsif.2010.0142

[13] M. A. Safi and A. B. Gumel, "Mathematical analysis of a disease transmission model with quarantine, isolation and an imperfect vaccine," *Computers & Mathematics with Applications*, vol. 61, no. 10, pp. 3044–3070, 2011. DOI:10.1016/j.camwa.2011.03.095

[14] B. D. Handari *et al.*, "An optimal control model to understand the potential impact of the new vaccine and transmission-blocking drugs for malaria: A case study in papua and west papua, indonesia," *Vaccines*, vol. 10, no. 8, p. 1174, 2022. DOI:10.3390/vaccines10081174

[15] D. Aldila *et al.*, "A tuberculosis epidemic model as a proxy for the assessment of the novel m72/as01e vaccine," *Communications in Nonlinear Science and Numerical Simulation*, vol. 120, p. 107162, 2023. DOI:10.1016/j.cnsns.2023.107162

[16] H. A. Fatahillah and D. Aldila, "Forward and backward bifurcation analysis from an imperfect vaccine efficacy model with saturated treatment and saturated infection," *Jambura Journal of Biomathematics (JJBM)*, vol. 5, no. 2, pp. 132–143, 2024. DOI:10.37905/jjbm.v5i2.28810

[17] D. Aldila, C. A. Puspadani, and R. Rusin, "Mathematical analysis of the impact of community ignorance on the population dynamics of dengue," *Frontiers in Applied Mathematics and Statistics*, vol. 9, p. 1094971, 2023. DOI:/10.3389/fams.2023.1094971

[18] O. Diekmann, J. A. P. Heesterbeek, and M. G. Roberts, "The construction of next-generation matrices for compartmental epidemic models," *Journal of the Royal Society Interface*, vol. 7, no. 47, pp. 873–885, 2009. DOI:10.1098/rsif.2009.0386

[19] D. Aldila *et al.*, "An analytical transmission model for evaluating pneumonia vaccination and control strategies," *Healthcare Analytics*, vol. 7, p. 100394, 2025. DOI:10.1016/j.health.2025.100394

[20] D. Aldila *et al.*, "Evaluating vaccination and quarantine for measles intervention strategy in jakarta, indonesia through mathematical modeling," *Partial Differential Equations in Applied Mathematics*, vol. 14, p. 101191, 2025. DOI:10.1016/j.padiff.2025.101191

[21] D. Aldila *et al.*, "Reassessment of public awareness and prevention strategies for hiv and covid-19 co-infections through epidemic modeling," *PLOS ONE*, vol. 20, no. 7, pp. 1–37, 2025. DOI:10.1371/journal.pone.0328488

[22] D. Aldila, "Change in stability direction induced by temporal interventions: a case study of a tuberculosis transmission model with relapse and reinfection," *Frontiers in Applied Mathematics and Statistics*, vol. 11, 2025. DOI:10.3389/fams.2025.1541981

[23] D. Aldila, "Optimal control for dengue eradication program under the media awareness effect," *International Journal of Nonlinear Sciences and Numerical Simulation*, vol. 24, no. 1, pp. 95–122, 2023. DOI:10.1515/ijnsns-2020-0142

[24] D. Aldila *et al.*, "Optimal control of pneumonia transmission model with seasonal factor: Learning from jakarta incidence data," *Heliyon*, vol. 9, no. 7, p. e18096, 2023. DOI:10.1016/j.heliyon.2023.e18096

[25] D. Aldila *et al.*, "Forward Bifurcation with Hysteresis Phenomena from Atherosclerosis Mathematical Model," *Communication in Biomathematical Sciences*, vol. 4, no. 2, pp. 125–137, 2021. DOI:10.5614/cbms.2021.4.2.4

[26] O. Diekmann, J. A. P. Heesterbeek, and M. G. Roberts, "The construction of next-generation matrices for compartmental epidemic models," *Journal of the Royal Society Interface*, vol. 7, no. 47, pp. 873–885, 2010. DOI:10.1098/rsif.2009.0386

[27] C. Castillo-Chavez and B. Song, "Dynamical models of tuberculosis and their applications," *Mathematical Biosciences and Engineering*, vol. 1, no. 2, pp. 361–404, 2004. DOI:10.3934/mbe.2004.1.361

[28] C. K. Mahadhika and D. Aldila, "A deterministic transmission model for analytics-driven optimization of covid-19 post-pandemic vaccination and quarantine strategies," *Mathematical Biosciences and Engineering*, vol. 21, no. 4, pp. 4956–4988, 2024. DOI:10.3934/mbe.2024219

[29] S. Marino *et al.*, "A methodology for performing global uncertainty and sensitivity analysis in systems biology," *Journal of Theoretical Biology*, vol. 254, no. 1, pp. 178–196, 2008. DOI:10.1016/j.jtbi.2008.04.011

[30] Z. Chazuka *et al.*, "Strategic approaches to mitigating Hookworm infection: An optimal control and cost-effectiveness analysis," *Results in Control and Optimization*, vol. 17, p. 100477, 2024. DOI:10.1016/j.rico.2024.100477

[31] A. H. Hassan *et al.*, "An Optimal Control Problem for a Monkeypox Transmission Model with Activity-Driven Contact Patterns," *Brazilian Journal of Physics*, vol. 55, no. 5, p. 213, 2025. DOI:10.1007/s13538-025-01844-4

[32] C. W. Chukwu *et al.*, "Exploring the epidemiological impact of Pneumonia–Listeriosis co-infection in the human population: a modeling and optimal control study," *International Journal of Dynamics and Control*, vol. 13, p. 197, 2025. DOI:10.1007/s40435-025-01714-6

[33] C. M. Kribs-Zaleta and J. X. Velasco-Hernández, "A simple vaccination model with multiple endemic states," *Mathematical Biosciences*, vol. 164, no. 2, pp. 183–201, 2000. DOI:10.1016/S0025-5564(00)00003-1

[34] D. Aldila *et al.*, "Backward bifurcation and periodic dynamics in a tuberculosis model with integrated control strategies," *Mathematical Biosciences and Engineering*, vol. 22, no. 10, pp. 2720–2760, 2025. DOI:10.3934/mbe.2025100

[35] W. Wang and S. Ruan, "Bifurcations in an epidemic model with constant removal rate of the infectives," *Journal of Mathematical Analysis and Applications*, vol. 291, no. 2, pp. 775–793, 2004. DOI:10.1016/j.jmaa.2003.11.043